Journal of Hazardous Materials 192 (2011) 222–225

Contents lists available at ScienceDirect

Journal of Hazardous Materials

journal homepage: www.elsevier.com/locate/jhazmat

Characteristics and the behavior in electrostatic precipitators of high-alumina coal fly ash from the Jungar power plant, Inner Mongolia, China

Qi Liqiang*, Yuan Yongtao

Environment Science and Engineering School, North China Electric Power University, Baoding 071003, China

ARTICLE INFO

Article history:
Received 27 December 2010
Received in revised form 3 May 2011
Accepted 4 May 2011
Available online 11 May 2011

Keywords:
High-alumina coal fly ash
Size distribution
Resistivity
Cohesive force
ESP

ABSTRACT

In China, flue gases emitted by coal-fired power plants are mainly cleaned using electrostatic precipitators (ESPs). However, based on observations, there is a decrease in the collection efficiency of ESPs in some power plants after burning Jungar coal in Inner Mongolia. In order to find the mechanism of coal fly ash escaping from ESPs, the size distribution, resistivity, and cohesive force of particulate matter samples from Jungar coal-fired power plants in China were measured using a Bahco centrifuge, a dust electrical resistivity test instrument, and a cohesive force test apparatus invented by the authors. Experiments were carried out to determine the chemical composition and current–voltage curve of fly ash under operating ESPs. The Al_2O_3 content in fly ash was found to reach more than 50%, with the size distribution showing a higher content of PM2.5 and PM10 in high-alumina coal fly ash than in other coal fly ashes. The resistivity of high-alumina coal fly ash was recorded at over 10^{12} Ω cm, but this did not result in a clear back corona. The cohesive force of high-alumina coal fly ash was very little. It was sensitive to smoke speed in the electric field, facilitating dust re-entrainment.

1. Introduction

Air pollution is a serious environmental problem worldwide, especially in developing countries like China [1]. Coal, one of the most abundant energy sources in China, is believed to remain as the major type of energy that will be in demand in the next several decades. The demand for coal as a major energy resource in the country is also projected to increase in the near future. Coal-fired power plants consume about 45% of the total annual coal consumption and are predicted to account for 62% of the same by 2010 [2,3]. According to a report released by the Coal Industrial Society of China in January 2009, China produced a total of about 2.716 billion tons of coal in 2008, which is 7.65% higher than that in 2007. Chinese power plants consumed 1.09 billion tons of coal and generated 81.8% of the total electricity in 2005. Meanwhile, 293 million tons of coal combustion residues were generated by Chinese power plants in 2005, and this amount is likely to increase every year [4].

An electrostatic precipitator (ESP) is a particulate control device used in modern pulverized-coal-fired power plants and in the cement industry to collect fly ashes from flue gas. As compared to a mechanical ash separator such as gravitational settling and cyclone, ESP achieves high overall mass collection efficiency, which is usually above 99% [5,6]. However, in China, there has been a decrease in the collection efficiency of ESPs in some power plants (Jungar 96.9%, Tuoketuo 96.7%) after burning Jungar high-alumina coal in Inner Mongolia. The fly ash from the Jungar power plant in Inner Mongolia, China is unique because it has a high concentration of alumina ($Al_2O_3 > 50\%$).

In this paper, the characteristics of the particulate matter emitted by Jungar high-alumina coal-fired power plants in China, including its size distribution, resistivity, and cohesive force have been analyzed for the first time. And the mechanisms of high-alumina coal fly ash as it escapes from ESPs have been preliminarily revealed.

2. Experimental

2.1. Samples

The ESPs in the Jungar, Tuoketuo, Zou Xian, and Shouyangshan power plants all have five electric fields through which flue gas passes before it is emitted into the atmosphere.

Samples 1–4 were collected directly from the flue gas at the entrance of the ESPs in the Jungar, Tuoketuo, Zou Xian, and Shouyangshan power plants. They were gathered in a filter drum and then stored in a reagent bottle (Table 1).

2.2. Experimental methods

The resistivity (lab and in situ) was experimented using the dust electrical resistivity test instrument invented by self-independence. If the resistivity is too low, below 10^4 Ω cm, the

* Corresponding author. Tel.: +86 13933270460; fax: +86 312 7522062.
E-mail address: qi_liqiang@163.com (L. Qi).

0304-3894/$ – see front matter
doi:10.1016/j.jhazmat.2011.05.012

Table 1
Sample description.

Sample	Sampling point	Source	Boiler	Precipitator and efficiency
1	Entrance of the ESP	Jungar power plant	1025 t/h pulverized coal-fired boiler	ESP; 96.9%
2	Entrance of the ESP	Tuoketuo power plant	2028 t/h pulverized coal-fired boiler	ESP; 96.7%
3	Entrance of the ESP	Zou Xian power plant	1025 t/h pulverized coal-fired boiler	ESP; 99.5%
4	Entrance of the ESP	Shouyangshan power plant	1025 t/h pulverized coal-fired boiler	ESP; 99.6%

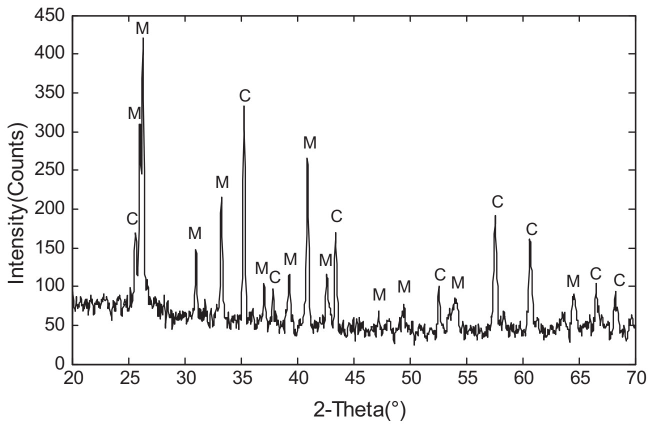

Fig. 1. XRD pattern of the Tuoketuo fly ash (M, mullite; C, Al_2O_3).

Table 2
Particle size distribution (%).

Sample	PM2.5	PM10
1	8.6	36.5
2	7.8	35.6
3	4.4	28.5
4	3.8	26.7

particles reaching the collecting electrode rapidly lose their charge and become re-entrained in the gas. On the other hand, if the resistivity is too high, above $10^{10}\,\Omega$ cm, the particles find it difficult to charge, thus limiting power input. The particles also become slow in losing their charge when they reach the collecting electrode because of the low conductivity of the particle layer that is already deposited. This increases the voltage gradient across the deposited layer, reduces the charging and collecting fields, and decreases the velocity of particle migration. If the particulate is very resistive or if it accumulates to a level that is considered high, the voltage gradient across the particle layer causes a dielectric breakdown and the back corona phenomenon, in which ions of opposite charges generated at the discharge electrode effectively neutralize the unipolar space charge and significantly reduce collection efficiency [7,8].

The size distributions were measured with a Bahco centrifuge.

Cohesive force test apparatus invented by self-independence was used to analyze the cohesive force of particulate matter samples. The adhesiveness of fly ash is an important factor in determining the characteristics of ESP; it influences the collection efficiency of ESP. The adhesive characteristic of fly ash allows its small particles to easily adhere and aggregate in order to be separated or collected easily, and they agglomerate into a shell structure to alleviate secondary dust when cleaning fly ash [9].

Particle mineralogy was examined by Y-2000 X-ray powder diffractometer (XRD). Accurate knowledge of the mineralogical composition of the fly ashes is useful for optimizing the removal of the fly ashes and for interpreting the mechanisms escaping from the ESP, as well as the abrasion of the boiler tubes and other parts of the power plants [10].

3. Results and discussion

3.1. Size distribution

Size distribution is one of the most important physical characteristics of particulate matter. A Bahco centrifuge measures the distribution of Stokes diameters. In this study, the distributions of PM10 (particles <10 μm in diameter) and PM2.5 (hazardous particulate matter with a mass median aerodynamic diameter of less than 2.5 μm) in the different samples were analyzed. Table 2 gives the particle size distribution data.

The results showed that the proportion of fine particles is greater in the downstream electric fields, indicating that the efficiency for collecting smaller particles is lower than that for larger particles. This can be attributed to the decreasing particle charging capacity of ESP in line with the decreasing particle diameters, based on the particle charging theory, and the increase in mobility along with the decreasing size (due to reduced drag force), which results in an offsetting of the reduced charge. For samples 1 and 2, PM10 and

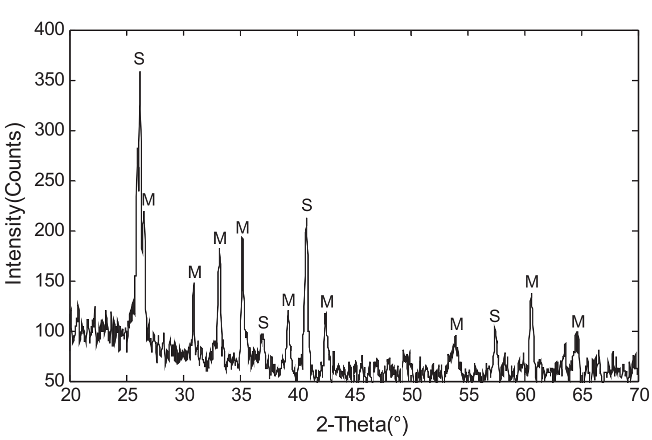

Fig. 2. XRD pattern of Shouyangshan fly ash (M, mullite; S, SiO_2).

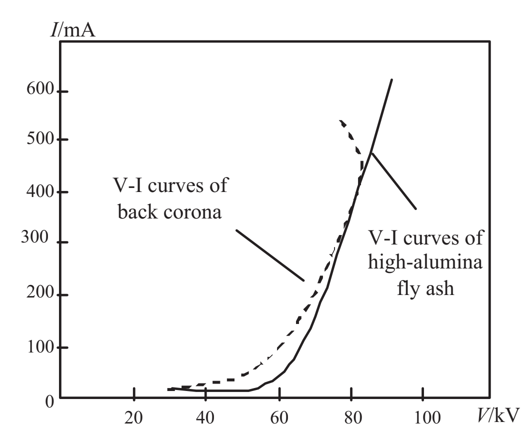

Fig. 3. The volt–ampere characteristic curves.

Table 3
Resistivity and chemical composition of samples 1–4.

Sample	SiO_2 (%)	Al_2O_3 (%)	Fe_2O_3 (%)	CaO (%)	MgO (%)	Unburned carbon (%)	Resistivity (Ω cm) (at 130 °C)
1	37.35	53.62	2.32	1.36	1.23	4.31	2.0×10^{12}
2	35.67	55.02	3.02	1.11	0.63	4.78	8.6×10^{12}
3	53.96	36.89	5.12	2.09	1.37	3.36	2.2×10^{11}
4	54.54	29.91	4.82	2.92	1.60	1.98	5.7×10^{10}

PM2.5 are clearly in a higher proportion, making ESP's efficiency relatively low.

3.2. Electrical resistivity and chemical composition

As is well known the efficiency of an ESP strongly depends on the resistivity of fly ash. Particle resistivity refers to the condition of particles in a gas stream that can alter the actual collection efficiency of an ESP design. The most economical design and operation of ESP are obtained when the electrical resistivity of the particulate is kept within certain limits. Resistivity refers to the resistance of the collected particle layer to the flow of electric current. It is the electrical resistance of a 1 cm^2 particle sample in a cross-sectional area that is 1 cm thick and recorded in unit Ω cm. It can be described as the resistance to the charge transfer of particles. Particle resistivity values can be classified into three regimes: low resistivity (up to say 10^4 Ω cm), normal resistivity (from 10^4 to 2×10^{10} Ω cm), and high resistivity (above 2×10^{10} Ω cm) [11].

The resistivity and chemical composition of different coal fly ashes are shown in Table 3.

In Table 3, the primary chemical components were SiO_2, Al_2O_3, Fe_2O_3, CaO, MgO and unburned carbon. And the resistivity was measured at 130 °C. The experimental results shown that the content of unburned carbon was lower than 5% in all samples, which had not obvious influence on the resistivity of the fly ash and the collection efficiency of the ESP [12–14]. In samples 1 and 2, the content of Al_2O_3 is much more than the other samples and the two samples have relatively high resistivity.

To maximize particle collection efficiency in electrostatic precipitators, the resistivity should be in the normal resistivity region. Resistivity is affected by factors such as the chemical composition of particles, water vapor, gas temperature, particle size, gas conditioning agents, and others. Among these, chemical composition of particles is the primary factor influencing resistivity problems effectively.

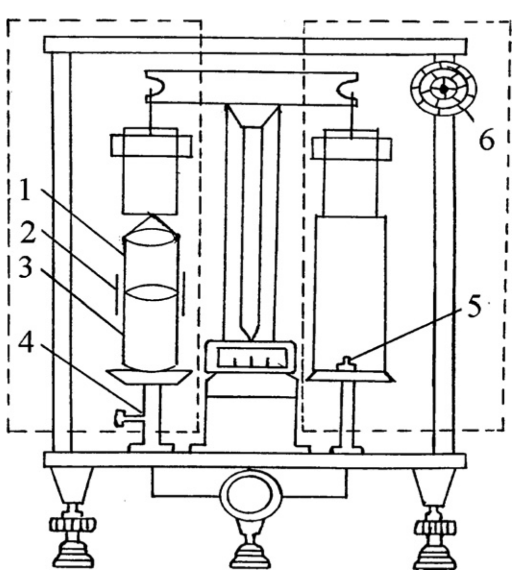

Fig. 4. The installation measuring cohesive force.

Table 4
The adhesive force of samples 1–4.

Sample	Adhesive force (mg/cm^2)
1	33.2
2	31.8
3	67.4
4	71.3

3.3. Mineralogical composition of the ashes

Two fly ash samples were analyzed from the Tuoketuo power plant (sample 2) and Shouyangshan power plant (sample 4). For the mineralogical analysis an X-ray diffractometer was used. X-ray diffraction patterns were collected at ambient temperature on a Philips X'Pert System, using a Y-2000 controlled diffractometer, with Cu graphite monochromatised radiation ($\lambda = 1.54178$ Å) with 1° scattering slit, a 2θ step of 0.03° and 1 s by step (2θ between 20° and 70°). The XRD patterns were shown in Figs. 1 and 2.

As shown in Figs. 1 and 2, minerals in Tuoketuo (high-alumina coal) fly ashes identified by XRD include mullite ($3Al_2O_3{\cdot}2SiO_2$), corundum (crystal Al_2O_3), quartz, and minor amounts of calcite and K-feldspar. But the mullite and quartz contents in Shouyangshan fly ashes are much lower than those in Tuoketuo fly ashes, in particular, the corundum (crystal Al_2O_3) contents are almost zero. Corundum is the perfect isolator, and mullite is also the material with high specific resistivity, so the high-alumina coal fly ash is difficult to charge and collect by ESP.

In Tuoketuo fly ashes, the aluminum compounds include mainly mullite ($3Al_2O_3{\cdot}2SiO_2$) and corundum (crystal Al_2O_3), but part of Al_2O_3 in the ash is in the form of tiny amorphous body. The pieces with fine granularity and less density and other compositions in the ash make it active during absorbing or releasing the charges especially the existence of carbon particles, so it is different from the familiar dust with high resistivity, and the back corona is inexistent at the ash surface on the unstriked pole plate after stopping the boiler operation. Because they can charge slowly under the condition of the strong electric field, then release the charges easily and obtain the positive charges through induction after aggradation. It is easy to re-entry airflow to form the secondary dust under the condition of the static force of plate. All of these cause the quick addition of corona current.

3.4. The volt–ampere (V–I) characteristic of high-alumina coal fly ash

Because the particles form a continuous layer on the ESP plates, all the ion currents must pass through the layer to reach the ground plates. This current creates an electric field in the layer, and it can become large enough to cause local electrical breakdown. When this occurs, new ions of the wrong polarity are injected into the wire–plate gap where they reduce the charge on the particles and may cause sparking. This breakdown condition is called "back corona".

The physical phenomena of a back corona are always the same: a lower spark-over voltage, a higher current flow, and a loss of collecting efficiency. The particle layer on the collection plate breaks down electrically, which produces small craters and visible back corona discharges occur. A back corona reduces the spark-over voltage, and thereby narrows the voltage interval within which the unit can be operated. The formation of the positive-ion current leads to a rapid increase in the slope of the voltage–current characteristic.

The voltage–current curve of the corona is particularly important for operation of EPS. It gives relations between the corona current and voltage.

According to the electric characteristic of ESP, its volt–ampere characteristic curve is different from the curves for fly ash of the coal-fired boiler with high specific resistivity. The results are shown in Fig. 3.

For typical high resistivity fly ash, when the back corona discharges occur, its voltage–current curve will appear an inflexion point at 80–100 kV, as shown by the dotted line in Fig. 3.

From Fig. 3, the beginning change of the curve (solid line) for electrostatic precipitator collected high-alumina coal fly ash is gentle and continuous with little slope and the change of the current quickens when the voltage achieves certain scale, while the familiar curve is always gentle although the current rises with the voltage rising till the breakdown is caused at certain high voltage in the two curves. There is not the back corona inflexion on the curve for high-alumina fly ash. And the back corona inflexion of ash layer at the breakdown is inexistent at the ash surface on the unstriked pole plate after stopping the boiler operation. The experiments about the volt–ampere characteristic for heating-operation electrostatic precipitator collected high-alumina fly ash show that the obvious back corona is not observed easily during operating and doing experiments.

3.5. The adhesive character of fly ash

The normal pull rift method was adopted [15], and a new installation that measures adhesive force was developed with reference to the fly ash in power plants (Fig. 4).

From Fig. 4, the primary part of the installation is modified due to TG328A analytical balance. The balance left is the sample section including up-silo (1), down-silo (3), caliper (2), adjustable bracket (4), etc. This is the hardcore part of installation. The right is the weight tray section including poise tray (5), ring poise tray (6), poises and ring poises. The walls and pontes of up-silo and down-silo with the same stainless steel material and the same specification are slick and inosculate accurately. The bottom of down-silo is sealed and the cross section is designed to the certain value “S” by experimental optimization. The caliper is made of two arc workpieces for fixing the up-silo and the down-silo together, so it must be installed or disconnected conveniently for keeping the silos integrate. The bracket is to adjust the silo height: the both sides of the balance are balanceable when the left hangs the silo with no sample. The two silos will separate when the certain poises and ring poises are put into the weight tray, and the uprightness-snap force can be calculated according to this weight.

The fly ashes was griddled at 80 μm and compared with the adhesive character of the other samples with alumina content. The results are shown in Table 4.

The Al_2O_3 content in samples 1 and 2 is higher than that in the other samples. Furthermore, the adhesive force of samples 1 and 2 is lower than that in half of samples 3 and 4. Thus, the Al_2O_3 content in fly ash may negatively affect the adhesive force in powder form.

The surface free energy in powder form is important to the adhesive force of particles. The higher the surface free energy in the solid form is, the weaker the adhesive force. The free energy in the solid state is needed to form the unit surface area, which can be confirmed through the solid’s melting point. The melting point of ashes increases when more and more multi-aluminum andalusites emerge with an increasing Al_2O_3 content. The conclusion is that the higher the Al_2O_3 content is, the weaker the adhesive character because the melting point can influence the free energy.

Thus, high-alumina fly ash does not necessarily cause a clear back corona of ESP, although its adhesive force is weaker. It is also sensitive enough to gas velocity in the electric field, which can in turn result in re-entrainment.

4. Conclusions

This study used high-alumina fly ash as sample and studied its entry in an operating ESP. After measuring and analyzing the resistivity and adhesive force of high-alumina fly ash, the results showed that when the Al_2O_3 content of fly ash is more than 50%, its resistivity reaches over 10^{12} Ω cm. This resistivity increases along with an increase in Al_2O_3 content. Meanwhile, the voltage–current curves showed that there is no clear reverse corona during the operation of ESP or while doing the experiments. The adhesive force of high-alumina fly ash is weaker, while its surface free energy is greater. It is also sensitive enough to gas velocity in the electric field, causing a re-entrainment, which in turn decreases the efficiency of ESPs.

Acknowledgements

This work was supported by the Natural Science Foundation of Hebei Province (Grant No. E2009001405) and the Fundamental Research Funds for the Central Universities (Grant No. 10MG36).

References

[1] H.H. Yi, J.M. Hao, X.L. Tang, Atmospheric environmental protection in China: current status, developmental trend and research emphasis, Energy Policy 35 (2007) 907–915.
[2] Q. Yao, S.Q. Li, H.W. Xu, et al., Studies on formation and control of combustion particulate matter in China: a review, Energy 34 (2009) 1296–1309.
[3] H.H. Yi, J.M. Hao, L. Duan, X. Li, X. Guo, Characteristics of inhalable particulate matter concentration and size distribution from power plants in China, J. Air Waste Manage. 56 (2006) 1243–1251.
[4] S.F. Dai, L. Zhao, S.P. Peng, et al., Abundances and distribution of minerals and elements in high-alumina coal fly ash from the Jungar power plant, Inner Mongolia, China, Int. J. Coal Geol. 81 (2010) 320–332.
[5] H.B. Zhao, C.G. Zheng, A stochastic simulation for the collection process of fly ashes in single-stage electrostatic precipitators, Fuel 87 (2008) 2082–2089.
[6] U. Shah, C. Zhang, J. Zhu, Comparison of electrostatic fine powder coating and coarse powder coating by numerical simulations, J. Electrostat. 64 (2006) 345–354.
[7] C.F. Zhang, Q. Yao, J.M. Sun, Characteristics of particulate matter from emissions of four typical coal-fired power plants in China, Fuel Process. Technol. 86 (2005) 757–768.
[8] G.L. Fisher, B.A. Prentice, D. Siberman, et al., Physical and morphological studies of size-classified coal fly ash, Environ. Sci. Technol. 12 (1978) 447–451.
[9] J. Dalmon, D. Tidy, The cohesive properties of fly ash in electrostatic precipitation, Atmos. Environ. 6 (1992) 81–92.
[10] G. Kostakis, Characterization of the fly ashes from the lignite burning power plants of northern Greece based on their quantitative mineralogical composition, J. Hazard. Mater. 166 (2009) 972–977.
[11] B. Wilhelm, Dust Extraction Technology, Technicopy Ltd., Glos, England, 1973.
[12] R. Barranco, M. Gong, A. Thompson, et al., The impact of fly ash resistivity and carbon content on electrostatic precipitator performance, Fuel 86 (2007) 2521–2527.
[13] H. Fujimura, A. Zukeran, Y. Ehara, et al., Influence on visibility index of re-entrainment phenomena in electrostatic precipitator, J. Aerosol Sci. 29 (1998) 483–484.
[14] Y.T. Yuan, Y. Zhao, J.P. Zhang, Effect of coal rank for the different coalification on the electric conductivity of fly ash, China Environ. Sci. 17 (1997) (in Chinese).
[15] National Standards of Peoples Republic of China: Method of Dust Character Test – Part 9: Determination of Cohesion-normal Pull Rift Method, GB/T16913.9-2008.